DMD Fast Forward. Published on September 30, 2024 as DOI: 10.1124/dmd.124.001867
This article has not been copyedited and formatted. The final version may differ from this version.

CYP and non-CYP drug metabolizing enzyme families exhibit differential sensitivities towards pro-inflammatory cytokine modulation

Laura M. de Jong, Chandan Harpal, Dirk-Jan van den Berg, Menno Hoekstra, Nienke J. Peter, Robert Rissmann, Jesse J. Swen and Martijn L. Manson

Division of Systems Pharmacology and Pharmacy, Leiden Academic Centre for Drug Research, Leiden University, Leiden, The Netherlands (L.M.J., C.H., D.J.B., M.H., N.J.P, M.L.M)

Department of Clinical Pharmacy and Toxicology, Leiden University Medical Center, Leiden, The Netherlands (J.J.S)

Centre for Human Drug Research, Leiden, Netherlands (R.R.)

Division of Biotherapeutics, Leiden Academic Centre for Drug Research, Leiden University, Leiden, The Netherlands (R.R.)

Department of Dermatology, Leiden University Medical Center, Leiden, The Netherlands (R.R.)

DMD Fast Forward. Published on September 30, 2024 as DOI: 10.1124/dmd.124.001867
This article has not been copyedited and formatted. The final version may differ from this version.

Running title: Impact of inflammation on drug metabolizing enzymes

Correspondence to: Martijn L. Manson. Division of Systems Pharmacology and Pharmacy, Leiden Academic Centre for Drug Research, Leiden University, Leiden, The Netherlands

Einsteinweg 55, 2333 CC Leiden, The Netherlands

Phone: +31 71 527 4400

Email: m.l.manson@lacdr.leidenuniv.nl

Number of Pages: 39

Number of Tables: 3

Number of Figures: 5

Number of References: 57

Number of Words in Abstract: 250

Number of Words in Introduction: 589

Number of Words in Discussion: 1198

List of abbreviations:

ACTB (β-actin), AhR (aryl hydrocarbon receptor), ANOVA (analysis of variance), CAR (constitutive androstane receptor), CESs (carboxylesterases), CYP (cytochrome P450), DMEs (drug metabolizing enzymes), DMSO (dimethyl sulfoxide), FBS (fetal bovine serum), FMOs (flavin monooxygenases), FOXA1 (forkhead box protein A1), FXR (farnesoid X receptor), GAPDH (glyceraldehyde-3-phosphate dehydrogenase), HNF1α (hepatocyte nuclear factor 1α), HNF4α (hepatocyte nuclear factor 4α), IC_{50} (half-maximal inhibitory concentration), IVIVE (*in vitro* to *in vivo* extrapolation), I_{max} (maximal inhibition), K_m

(Michaelis-Menten constant), LC-MS/MS (liquid chromatography-mass spectrometry), LXRα (liver X receptorα), NFY (nuclear factor Y), Nrf2 (nuclear factor E2-related factor 2), Pen/Strep (Penicillin/Streptomycin), PBPK model (physiologically based pharmacokinetic model), PHH (primary human hepatocyte), PPARα (peroxisome proliferator activated receptor α), PXR (pregnane X receptor), RPLP0 (ribosomal protein lateral stalk subunit P0), RT-qPCR (reverse transcription-quantitative polymerase chain reaction), SULTs (sulfotransferases), UGTs (UDP glucuronosyltransferases), USF1 (upstream transcription factor 1), VDR (vitamin D receptor).

Abstract

Compromised hepatic drug metabolism in response to pro-inflammatory cytokine release is primarily attributed to downregulation of cytochrome P450 (CYP) enzymes. However, whether inflammation also affects other phase I and phase II drug metabolizing enzymes (DMEs) like the flavin monooxygenases (FMOs), carboxylesterases (CESs) and UDP glucuronosyltransferases (UGTs) remains unclear. This study aimed to decipher the impact of physiologically relevant concentrations of pro-inflammatory cytokines on expression and activity of phase I and phase II enzymes, in order to establish a hierarchy of their sensitivity as compared to the CYPs. Hereto, HepaRG cells were exposed to interleukin-6 and interleukin-1β to measure alterations in DME gene expression (24h) and activity (72h). Sensitivity of DMEs towards pro-inflammatory cytokines was evaluated by determining IC_{50} (potency) and I_{max} (maximal inhibition) values from the concentration-response curves. Pro-inflammatory cytokine treatment led to nearly complete downregulation of *CYP3A4* (~98%), but was generally less efficacious at reducing gene expression of the non-CYP DME families. Importantly, FMO, CES and UGT family members were less sensitive towards interleuking-6 induced inhibition in terms of potency, with IC_{50} values that were 4.3-7.4 fold higher than *CYP3A4.* Similarly, 18- to 31-fold more interleukin-1β was required to achieve

DMD Fast Forward. Published on September 30, 2024 as DOI: 10.1124/dmd.124.001867
This article has not been copyedited and formatted. The final version may differ from this version.

50% of the maximal downregulation of *FMO3, FMO4, CES1, UGT2B4 and UGT2B7* expression. The differential sensitivity persisted at enzyme activity level, highlighting that alterations in DME gene expression during inflammation are predictive for subsequent alterations in enzyme activity. In conclusion, we have shown that FMOs, CES and UGTs enzymes are less impacted by IL-6 and IL-1β treatment as compared to CYP enzymes.

Significance statement

While the impact of pro-inflammatory cytokines on CYP expression is well established, their effects on non-CYP phase I and phase II drug metabolism remains underexplored, particularly regarding alterations in drug metabolizing enzyme activity. This study provides a quantitative understanding of the sensitivity differences to inflammation between DME family members, suggesting that non-CYP DMEs may become more important for the metabolism of drugs during inflammatory conditions due to their lower sensitivity as compared to the CYPs.

DMD Fast Forward. Published on September 30, 2024 as DOI: 10.1124/dmd.124.001867
This article has not been copyedited and formatted. The final version may differ from this version.

Introduction

Inflammation is increasingly recognized as a contributor to the regulation and variability of drug clearance in humans, presumably due to alterations in drug metabolism (Stanke-Labesque et al. 2020; Dunvald et al. 2022). More specifically, the widespread elevation of pro-inflammatory cytokines such as IL-6 and IL-1β affects gene expression of drug metabolizing enzymes (DMEs) in hepatocytes (Aitken and Morgan 2007; Dickmann et al. 2011; Dickmann et al. 2012; Klein and Zanger 2013; Tanner et al. 2018), subsequently affecting hepatic drug clearance and efficacy or safety of drug treatments (Leung et al. 2014). Considering the high prevalence of both acute and chronic inflammatory diseases, it is crucial to take into account how hepatic drug metabolism of both novel and existing drugs can be affected by inflammation.

In vitro studies using human liver models have been instrumental in broadening our understanding of inflammation-induced alterations in drug metabolism, and can facilitate in quantifying these effects. A promising approach to predict the subsequent impact of inflammation on drug clearance *in vivo* involves utilizing *in vitro* data coupled with physiologically based pharmacokinetic (PBPK) models. This approach has demonstrated its utility in predicting the influence of elevated IL-6 levels on drug clearance, particularly for substrates of the key DMEs CYP3A4 and CYP2C19 (Machavaram et al. 2013; Xu et al. 2015; Jiang et al. 2016; Lenoir et al. 2022; Stader et al. 2022). Generating more physiologically relevant quantitative *in vitro* data will likely aid in utilizing PBPK models to predict the impact of inflammation on drug clearance for substrates of other CYP enzymes and non-CYP mediated pathways (Ozbey et al. 2023).

Importantly, it is estimated that clearance of ~25% of the top 200 most prescribed small molecule drugs approved by the FDA is mainly dependent on non-CYP enzymes, with the UDP-glucuronosyltransferase (UGT) family contributing to biotransformation in 45% of the cases (Saravanakumar et al. 2019). However, whereas the impact of pro-inflammatory cytokines on CYP expression is well established, the potential impact on other DME families

including the UGTs, sulfotransferase (SULTs), flavin-containing monooxygenase (FMOs) and carboxylesterases (CESs) has received considerably less attention. Yet, it remains unclear to what extent the activity of non-CYP metabolizing enzymes is affected by inflammation, and whether these enzymes exhibit a comparable sensitivity to the effects of inflammatory cytokines as compared to the CYP enzymes.

Another limitation of available *in vitro* data is that they have mostly focused on the impact of cytokines on the mRNA expression levels of DME enzymes rather than on their enzymatic activity. While significant changes in the expression of DME mRNA during inflammation have indeed prompted focus on transcription as the primary mechanism underlying changes in metabolic capacity, there is increasing acknowledgment of the influence of post-transcriptional mechanisms on DME activity (Stanke-Labesque et al. 2020). Consequently, a strong up- or downregulation of mRNA expression observed upon cytokine stimulation may not necessarily translate into similar alterations in enzyme activity. Furthermore, *in vitro* studies are often conducted using cytokine concentrations that surpass the physiological concentrations observed in patients, compromising clinical translation (de Jong et al. 2020). IL-6 levels typically range from 10 to 1000 pg/ml during inflammatory conditions, and IL-1β can reach up to 50 pg/ml (Jablonska et al. 2001; Machavaram et al. 2013; Coutant and Hall 2018). However, most *in vitro* studies have exclusively examined the effects of 10 ng/ml IL-6 and 1 ng/ml IL-1β, concentrations that far exceed physiological levels. This underscores the necessity of investigating changes in enzymatic activity upon physiologically relevant concentrations of cytokines to generate reliable quantitative *in vitro* data.

In this study, we therefore investigated the concentration-dependent effects of IL-6 and IL-1β on both the mRNA expression and activity of CYP and non-CYP drug metabolizing enzymes in a relevant human hepatocarcinoma cell line, i.e. in HepaRG cells. Quantifying the impact of inflammatory mediators across various drug metabolizing enzyme families allowed us to establish a hierarchy of their sensitivity. By comparing the effects of IL-6 and IL-1β on transcription versus activity, we shed light on whether alterations in mRNA serve as a reliable

DMD Fast Forward. Published on September 30, 2024 as DOI: 10.1124/dmd.124.001867
This article has not been copyedited and formatted. The final version may differ from this version.

predictor of corresponding changes in enzyme activity during inflammation. This information is essential for enhancing our understanding of the impact of inflammation on drug metabolism and could be implemented in modeling tools aimed at optimizing drug dosing strategies for patients with inflammatory disease.

Material and Methods

Reagents and chemicals

William's E Medium with GlutaMAX™ Supplement and trypsin-EDTA (0.25%) was purchased from ThermoFisher (Waltham, MA, USA). Fetal bovine serum (FBS) was obtained from Merck (Batch number: 0001663799), penicillin/streptomycin (Pen/Strep) was obtained from Lonza (Basel, Switzerland). Hydrocortisone, dimethyl sulfoxide (DMSO), human insulin and primers were obtained from Sigma-Aldrich (St. Louis, Misouri, USA). Dulbecco's phosphate-buffered saline (D-PBS) was obtained from Capricorn Scientific (Ebsdorfergrund, Hessen, Germany). SensiMix SYBR Lo-ROX kit and 10x NH4 Reaction Buffer for RT-qPCR were purchased from Meridian BioScience (Cincinnati, Ohio, USA). Maxima H minus Reverse transcriptase and 5x RT buffer was purchased from Thermo Scientific (Waltham, MA, USA). Human recombinant IL-6 and human recombinant IL-1β were purchased from Peprotech (London, UK). All cytokines were reconstituted and stored as high concentration stocks according to the manufacturer's instructions. S-mephenytoin, 4′-hydroxymephenytoin, 4′-hydroxymephenytoin-d_3, diclofenac, 4'-hydroxydiclofac, 4'-hydroxydiclofenac-$^{13}C_6$, phenacetin, acetaminophen, benzydamine N-oxide and benzydamine N-oxide-d_6 were purchased from LGC (Wesel, Germany). Acetaminophen-d_4 was purchased from Alsachim (Illkirch-Graffenstaden, France). Benzydamine was purchased from Sigma-Aldrich (St. Louis, MO, USA). 1'-Hydroxymidazolam was purchased from Cerilliant (Round Rock, Texas, USA) and 1'-hydroxymidazolam-d_4 from Supelco (St. Louis, Misouri, USA). Midazolam hydrochloride, morphine, morphine-3-glucuronide and morphine-3-gluronide-d_3 were from

Duchefa Farma (Haarlem, the Netherlands). Acetonitrile, methanol, water and formic acid of LC-MS grade were obtained from Merk (Darmstadt, Germany).

HepaRG culture and treatment

HepaRG cells at passage 12 (batch HPR101067) were purchased from Biopredict International (Rennes, France) and expanded to set up a working bank according to the provider's instructions. Cells plated in 96-wells plates at a density of 9000 cells/well were first grown in William's E medium GlutaMAX supplemented with 10% FBS, 100 U/mL Pen/Strep, 5 µg/mL human insulin, and 20 mg/mL hydrocortisone for two weeks. Subsequently, cells were cultured for an additional two weeks in the same medium supplemented with 2% DMSO to get fully differentiated cells (Gripon et al. 2002). Cells were maintained at 37°C in 5% CO_2 throughout the experiment.

The FBS concentration in the DMSO-containing HepaRG medium was reduced to 1% at 24 hours before treatment with the cytokines IL-6 or IL-1β. Concentrations of IL-6 used for the experiments ranged from 0.0001 ng/mL to 10 ng/mL and from 0.001 pg/mL to 1 ng/mL for IL-1β, respectively. For gene expression analysis, cells were treated with IL-6 or IL-1β for 24 hours prior to lysis. For activity measurements, the cytokine-containing medium was renewed every 24 hours. After 72 hours, the medium was replaced by 2% DMSO-containing serum-free medium with a substrate specific to the DME of interest, as described in detail below. An CyQUANT LDH Cytotoxicity Assay (Thermo Scientific, Wilmington, US) was conducted after 72 hours to evaluate cytotoxicity at the highest concentrations of IL-6 and IL-1β, yielding cytotoxicity levels of 6% and 14%, respectively.

Human liver biopsies

Human liver biopsies were obtained from the gastroenterology biobank at the Leiden University Medical Center (LUMC, Leiden, the Netherlands), as described elsewhere (de Jong et al. 2023).

Reverse transcription-quantitative polymerase chain reaction (RT-qPCR)

DMD Fast Forward. Published on September 30, 2024 as DOI: 10.1124/dmd.124.001867
This article has not been copyedited and formatted. The final version may differ from this version.

Total RNA was isolated from HepaRG cells or human liver biopsies following the acid guanidinium thiocyanate-phenol-chloroform extraction, as described elsewhere (Chomczynski and Sacchi 1987). Concentration and purity of RNA was subsequently measured using a NanoDrop 3300 (Thermo Scientific, Wilmington, US). Synthesis of cDNA was performed with 0.5 µg RNA input using Maxima H Minus Reverse Transcriptase (Thermo scientific) according to the manufacturer's instructions. RT-qPCR analysis was performed with a QuantStudio™ 6 Flex System using SYBR Green technology. RT-qPCR samples were run in duplicate. All PCR primers were designed in-house and subsequently checked for amplification efficiency (Supplemental Table 1). Relative mRNA levels were calculated using the comparative ΔΔCt method (Livak and Schmittgen 2001).The expression in each HepaRG sample was normalized by subtracting the geometric mean Ct value of the endogenous control genes ribosomal protein lateral stalk subunit P0 (RPLP0), glyceraldehyde-3-phosphate dehydrogenase (GAPDH) and β-actin (ACTB) from the target Ct value to obtain the ΔCt (eq. 1)

$$\Delta\mathrm{Ct} = Ct(target) - Ct(RPLP0, GAPDH, ACTB) \quad (1)$$

Subsequent relative gene expression levels were calculated as $2^{-\Delta\mathrm{Ct}}$. Fold changes of treated cells as compared to PBS-control cells were calculated using eq. 2 and 3.

$$\Delta\Delta\mathrm{Ct} = \Delta\mathrm{Ct}(treated) - \Delta\mathrm{Ct}(PBS\ control) \quad (2)$$

$$Fold\ change = 2^{-\Delta\Delta\mathrm{Ct}} \quad (3)$$

Data are expressed as mean fold changes ± SEM. Basal gene expression in HepaRG cells and human liver biopsies presented in Fig. 1 and Supplemental Fig. 2 are exclusively normalized for *RPLP0*. This is due to the fact that *RPLP0* was identified as a stable endogenous control in liver biopsies, unlike other housekeeping genes (PMID: 37361233). Statistical analysis were carried out on ΔCT values, due to the considerable skewed symmetry of up- and downregulation in the linear fold change.

Drug metabolizing enzyme activities in HepaRG cells

Determination of DME activity was based on the metabolic conversion of probe substrates, i.e. midazolam for CYP3A4, phenacetin for CYP1A2, diclofenac for CYP2C9, S-mephenytoin for CYP2C19, benzydamine for FMO3, and morphine for UGT2B7 using liquid chromatography coupled to tandem mass spectrometry (LC-MS/MS). CYP2D6 activity could not be determined since HepaRG cells are derived from a CYP2D6 poor metabolizer patient and was thus excluded from our analysis (Guillouzo et al. 2007). Cells were exposed to 5 µM midazolam for 30 minutes, 50 µM phenacetin for 2 hours, 10 µM diclofenac for 2 hours, 100 µM S-mephenytoin for 2 hours, 10 µM benzydamine for 4 hours, or 100 µM morphine for 4 hours in serum-free William's E medium supplemented with 2% DMSO. Substrate concentrations were selected below the Michaelis-Menten constant (K_m) to achieve selective metabolic conversion by the specific DME isoform (Störmer et al. 2000; Court et al. 2003; Spaggiari et al. 2014). Afterwards, cell medium samples containing the probe substrates and their metabolites were collected and mixed with 250 mM formic acid, and immediately frozen at -20 degrees. Notably, UGT2B7 activity samples were mixed with 1 M sodium carbonate and then frozen. For quantification of the metabolites 1'hydroxymidazolam (CYP3A4), acetaminophen (CYP1A2), 4'hydroxydiclofenac (CYP2C9), 4'hydroxymephentoin (CYP2C19), benzydamine-N-oxide (FMO3) or morphine-3-glucuronide (UGT2B7) samples were subjected to LC-MS/MS based analysis. A detailed description of the LC-MS/MS analysis can be found in the Supplemental Methods 'LC-MS/MS method to quantify CYP activity' or 'LC-MS/MS method to quantify FMO3 and UGT2B7 activity', where MS-specific parameters are listed in Supplemental Table 2 and Supplemental Table 3. CES1 activity was not determined due to the absence of a probe-based analytical detection method. Enzyme activity data were normalized to the amount of cells per well and presented as the rate of metabolite formation in picomole/min/million cells as compared to untreated cells.

Statistical Analysis

Results were generated from at least four independent experiments. Relative half-maximal inhibitory concentrations (IC_{50}) of IL-6 and IL-1β for DME expression and activity were

DMD Fast Forward. Published on September 30, 2024 as DOI: 10.1124/dmd.124.001867
This article has not been copyedited and formatted. The final version may differ from this version.

determined using GraphPad Prism 9.2.0 software (GraphPad Software, La Jolla, CA, USA) through nonlinear regression on the basis of the four-parameter logistic function (Sebaugh 2011). In case the concentration-response curve did not reach the lower asymptote upon the highest cytokine stimulation, IC_{50} values were determined by directly interpolating from the studied concentration-response curve, without extrapolation for higher cytokine concentrations beyond the range of observed data points. Percentual maximal inhibition (I_{max}) values were calculated based upon the upper and lower asymptotes of the concentration-response curves. Statistical significance in IC_{50} and I_{max} values between DME isoforms was determined by the parametric one-way analysis of variance (ANOVA) test assuming normal distribution of data and applying the Dunnet's post hoc test for comparison to CYP3A4 in GraphPad Prism 9. Statistical significance between IC_{50} and I_{max} values on mRNA and activity was done using an unpaired t-test. The criterion was based on the P values and indicated with * P≤0.05, ** P≤ 0.01, *** P≤ 0.001 and NS, not significant.

DMD Fast Forward. Published on September 30, 2024 as DOI: 10.1124/dmd.124.001867
This article has not been copyedited and formatted. The final version may differ from this version.

Results

Basal mRNA expression of DMEs in HepaRG is comparable to human livers

The mRNA expression levels of four CYP enzymes (*CYP3A4*, *CYP2C9*, *CYP2C19*, *CYP1A2*), five other phase I enzymes (*FMO1*, *FMO3*, *FMO4*, *CES1*, *CES2*) and four phase II enzymes (*UGT1A4*, *UGT2B4*, *UGT2B7* and *UGT2B15*) were analysed by RT-qPCR in HepaRG cells and biopsies of human livers (Figure 1). Rank order of P450 expression was *CYP3A4* > *CYP2C9* > *CYP2C19* > *CYP1A2* in HepaRG cells and *CYP2C9* > *CYP3A4* > *CYP2C19* > *CYP1A2* in human livers. *CYP1A2* expression was relatively low in HepaRG as compared to human livers, consistent with previous characterization studies (Guillouzo et al. 2007). The rank order of other phase I enzymes expression was *FMO3* > *FMO4* > *FMO1* and *CES1* > *CES2*. For the included phase II enzymes, the expression order was UGT2B4 > UGT2B15 > UGT1A4 > UGT2B7. This pattern was consistent in both HepaRG cells and human livers, aligning with previous research (Hines 2006; Izukawa et al. 2009). Thus, the rank order within DME families exhibited strong similarity between human livers and the HepaRG cell model, suggesting that the HepaRG cell model is not only suitable for providing translation input regarding CYP enzymes but also for other DME families.

Impact of pro-inflammatory cytokine treatment on CYP expression and activity

The effect of inflammation on the gene expression and enzyme activity of selected phase I and phase II DMEs was evaluated by determining the IC_{50} (potency) and I_{max} (efficacy) values of IL-6 and IL-1β on individual isoforms.

DMD Fast Forward. Published on September 30, 2024 as DOI: 10.1124/dmd.124.001867
This article has not been copyedited and formatted. The final version may differ from this version.

A concentration-dependent decrease in the relative mRNA expression of all CYP isoforms was observed following treatment with both IL-6 and IL-1β. Among the CYP family members, no substantial differences were noted in the isoform-specific response to cytokine treatment, as evident from the comparable potency and efficacy values (Fig. 2A, Table 1). Comparison of IC_{50} values and maximum suppression values for IL-1β and IL-6 indicated that in general, IL-1β is much more potent than IL-6 in suppressing DME gene expression and enzyme activity. This finding corroborates previous research in HepaRG cells (Klein et al. 2015). We next examined whether the alterations at the DME gene expression level were retained at the enzyme activity level. Indeed, a concentration-dependent decrease was observed for CYP activity of all isoforms (Fig. 2B, Table 2). In contrast to the similar potencies of IL-6 and IL-1β in modulating expression levels of different CYP isoforms, there was a distinct potency difference (~10-fold) between the impact of inflammation on CYP2C19 and CYP2C9 enzyme activities as compared to CYP3A4 activity, which was reflected by a higher sensitivity of CYP3A4 activity towards IL-6 and IL-1β.

Non-CYP isoforms are differentially affected by cytokine treatment as compared to CYP isoforms

We next examined the impact of IL-6 and IL-1β treatment on the different members of the most important non-CYP DME families. Sensitivity differences in response to cytokine treatment amongst DME families were defined by benchmarking potency and efficacy values against CYP3A4, that is recognized as the most important DME in humans because of its clinical importance and high expression (Zanger and Schwab 2013). Interestingly, gene expression of *FMO3*, *FMO4*, *CES1*, *CES2*, *UGT1A4*, *UGT2B4* and *UGT2B7* was in terms of potency less sensitive towards the effects of IL-6 as compared to *CYP3A4*, with IC_{50} values that were 4 to 9 fold higher than for *CYP3A4* (Figure 3A, Table 1). Additionally, while IL-6 elicited a maximal downregulation of only 55 ± 9% for *FMO3*, 57 ± 4% for *FMO4*, 39 ± 15% for *CES1* and 48 ± 13% for *CES2*, it led to a nearly complete downregulation of 97 ± 1% for *CYP3A4* expression. This difference in efficacy of IL-6 was similarly observed across all

members of the *UGT* family, where maximal downregulation ranged from 60 ± 12% to 73 ± 7%.

Similar patterns were observed for the impact of IL-1β on non-CYP DME isoforms. *FMO3*, *FMO4*, *CES2*, *UGT2B4* and *UGT2B7* exhibited a significantly lower sensitivity to IL-1β as compared to *CYP3A4*, indicating that a, respectively, 18, 28, 30, 9 and 14- fold higher concentration of IL-1β was needed to exert 50% of the maximal downregulation by this cytokine. Interestingly, IL-1β did not impact *CES1* expression across all concentrations tested. In addition, the maximal inhibitory effect of IL-1β on gene expression levels of *FMO3*, *FMO4*, *CES2*, *UGT1A4* and *UGT2B7* ranged from 80 ± 3% to 84 ± 17%, which was less as compared to the observed near-complete downregulation of 99 ± 2% of *CYP3A4*.

Importantly, the differential potency and maximal inhibitory impact of inflammatory mediators on different members of the DME families could be confirmed at the enzyme activity level (Figure 3B, Table 2). Compared to CYP3A4 activity, FMO3 activity was less sensitive towards the effects of IL-6, as evident by a 26-fold difference in potency. UGT2B7 activity was even less sensitive towards IL-6, with a 35-fold difference in IC_{50} value as compared to CYP3A4 activity. In addition, maximal inhibition by IL-6 was only 29 ± 5% for FMO3, and 69 ± 7% for UGT2B7, significantly less than the maximal inhibition of 93 ± 2% that was observed for CYP3A4 activity. The maximal downregulation of FMO3 activity following IL-1β treatment was 54 ± 5%, which was also less than observed for the CYP3A4 activity (98 ± 1%). However, IL-1β showed comparable potency towards FMO3 activity inhibition as compared to CYP3A4 activity inhibition, highlighting that the efficacy of IL-1β rather than the sensitivity to IL-1β differed between FMO3 and CYP3A4 activities. UGT2B7 activity displayed lower sensitivity towards IL-1β, which was reflected by a 31-fold difference in IC_{50} value as compared to CYP3A4.

Transcriptional regulation is the main driver of the cytokine-mediated inhibition of DMEs

DMD Fast Forward. Published on September 30, 2024 as DOI: 10.1124/dmd.124.001867
This article has not been copyedited and formatted. The final version may differ from this version.

Several studies have suggested that inflammation-related post-transcriptional mechanisms may modulate CYP activity, which would theoretically result in a mismatch in the overall impact of inflammatory mediators in altering DME gene expression versus enzyme activity. To investigate whether post-transcriptional modifications induced by inflammation are indeed critical to the effect, acquired IC_{50} and I_{max} values for DME gene expression and enzyme activity were compared (Fig. 4). Overall, there was a strong linear relationship between the potency of IL-6 and IL-1β on DME expression and DME activity ($P < 0.0001$)(Fig. 4A). Importantly, 90% of the variability in DME activity could be explained by changes in transcription (R^2=0.9), highlighting the strong association between alterations in gene expression and enzyme activity during inflammation. We next compared individual expression versus activity IC_{50} values for CYP3A4, CYP2C19, CYP2C9, CYP1A2, FMO3 and UGT2B7, visually presented in Supplemental Figure 1. CYP3A4 activity was more sensitive towards IL-6 induced downregulation compared to *CYP3A4* expression, and this was similarly seen for FMO3 activity upon IL-1β treatment. In contrast, *CYP2C19* and *CYP2C9* expression was more sensitive towards IL-1β treatment as compared to CYP2C19 and CYP2C9 activity. For other isoforms, similar IC_{50} values on expression and activity level were found. The maximal impact of IL-6 and IL-1β on expression and activity of the DMEs was highly similar, except for the mismatches observed for FMO3 (Fig. 4B).

Comparison of IC_{50} values for cytokine-induced CYP changes in HepaRG cells versus 2D and 3D PHH models

To further highlight the translational value of the HepaRG cell line as *in vitro* liver model, we compared our quantitative cytokine-induced changes to what has been reported before in 2D and 3D PHH models (Dickmann et al. 2011; Dickmann et al. 2012; Klöditz et al. 2023). Comparing our HepaRG IL-6 IC_{50} values with those previously determined for CYP isoforms in 2D/3D PHHs showed good agreement between the results (Table 3). The potency of IL-6 in inducing transcriptional alterations in CYPs in 3D PHH spheroids was almost identical as compared to the potency found in HepaRG cells. The IC_{50} data acquired in a 2D PHH model

were also comparable. However, it should be noted that basal CYP expression rapidly declines in 2D cultures of PHH, even in the absence of a pro-inflammatory stimulus (Kiamehr et al. 2019). The correspondence of our HepaRG IC_{50} data does not hold so well for comparing the potency of IL-1β on CYP expression and activity in PHHs. Although we found the most pronounced effects on CYP3A4, similarly to the results in 3D PHHs, IL-1β was much more potent in HepaRG cells as compared to PHHs. This might in part be due to the morphological heterogeneity of HepaRG cells, where biliary-like cells release additional pro-inflammatory cytokines, amplifying the IL-1β response (Pinto et al. 2018). Indeed, aggravation of the IL-1β, but not the IL-6 response has been demonstrated in hepatocyte co-culture models as compared to hepatocytes alone, where a sensitivity increase up to 50-fold was observed for CYP3A4 (Nguyen et al. 2015). Taken together, these findings demonstrate that HepaRG cells exhibit comparable sensitivity to IL-6-induced transcriptional changes in CYP enzymes as observed in 2D and 3D PHH models.

Cytokine specific effects on nuclear receptors and transcription factors regulating the DMEs

Our data indicates that transcriptional alterations in DME are the primary mechanism underlying inflammation-related changes in CYP enzyme activity *in vitro*. To gain mechanistic insight into the differential regulation of hepatic gene expression by cytokines, we investigated the effects of IL-6 and IL-1β on a selection of nuclear receptors and transcription factors generally considered to be involved in DME gene expression regulation (Fig. 5). PXR and CAR are identified as key transcriptional regulators of the CYP enzymes, with confirmed binding sites in the response elements of human CYP3A4/5, CYP2C9, CYP2C19 and CYP1A2 (Xie et al. 2000; Ferguson et al. 2002; Chen et al. 2003). NFY and USF1 are essential for constitutive FMO3 transcription via promoter binding (Klick and Hines 2007), while LXRα has recently been identified as regulator of human CES (Collins et al. 2022). UGT family regulation is isoform-specific, with AhR and HNF1α implicated in UGT1A4 regulation, FXR and PPARα in UGT2B4 regulation, and Nrf2, FXR, HNF4α, HNF1, VDR, and

DMD Fast Forward. Published on September 30, 2024 as DOI: 10.1124/dmd.124.001867
This article has not been copyedited and formatted. The final version may differ from this version.

FOXA1 in the regulation of UGT2B7 and UGT2B15 (Hu et al. 2014). Basal gene expression of these regulators in HepaRG cells was confirmed with RT-qPCR (Supplemental Figure 2). PXR and CAR expression was most strongly downregulated, i.e. >60% by IL-6 treatment and >90% by IL-1β treatment. IL-1β also downregulated RXRα (~60%), LXRα (~80%), HNF1α (~80%), AhR (~50%), Nrf2 (~70%) and PPARα (~80%), which was not seen after IL-6 treatment. Expression of HNF4α was downregulated by ~70% following IL-1β treatment and ~40% by IL-6 treatment. The other regulators FXR, NFYA and USF1 were unaffected by both IL-6 and IL-1β. Sensitivity towards IL-6 and IL-1β was evaluated for PXR and CAR, as these regulators were most affected by cytokine treatment. The IC_{50} values for IL-6 treatment were 0.86 ± 0.46 ng/ml for PXR and 0.38 ± 0.56 ng/ml for CAR, while for IL-1β treatment, the IC_{50} values were 4.37 ± 3.68 pg/ml for PXR and 2.50 ± 7.41 pg/ml for CAR. Concentration-response curves for PXR and CAR as compared to one of the key genes they regulate, *CYP3A4*, is presented in Supplemental Figure 3.

DMD Fast Forward. Published on September 30, 2024 as DOI: 10.1124/dmd.124.001867
This article has not been copyedited and formatted. The final version may differ from this version.

Discussion

Pro-inflammatory cytokine release during inflammatory conditions is associated with compromised metabolism of drugs in the liver. The impact of pro-inflammatory cytokines on *in vitro* CYP expression is well-characterized (de Jong et al. 2020). However, less attention has been credited to the effects on non-CYP phase I and phase II drug metabolism, and especially data on the effects of inflammation on DME activity is lacking. Our results demonstrate that members of the non-CYP families FMOs, CESs and UGTs were less sensitive towards the effects of IL-6 and IL-1β as compared to the CYP family. This differential sensitivity was evident at both the DME gene expression and DME enzyme activity level, highlighting that alterations in transcription during inflammation are highly predictive for subsequent alterations in enzyme activity.

Our concentration-response experiments defined differences in both the potency and efficacy of cytokines in inducing downregulation of expression and activity of individual DME family members. While results from previous *in vitro* studies at supraphysiological concentrations of IL-6 have hinted towards a more limited impact on UGT isoforms as compared to CYP isoforms (Klein and Zanger 2013; Keller et al. 2016; Gramignoli et al. 2022), this study is the first to directly compare multiple DME families on both expression and activity. Rank ordering of DME sensitivity highlighted that CYP isoforms exhibited the highest sensitivity to the modulatory effects of IL-6 and IL-1β, whereas members from the FMO, CES and UGT family

consistently showed a lower sensitivity. Importantly, this differential sensitivity was observed for both IL-6 and IL-1β treatment, even though IL-6 and IL-1β induce different inflammatory signaling pathways (Weber et al. 2010; Schaper and Rose-John 2015) and exert different effects on transcriptional regulators (Klein et al. 2015).

The mechanisms underlying this differential sensitivity could stem from the differential impact of cytokines on the regulators of the DMEs. IL-6 and IL-1β stimulation of HepaRG cells profoundly and significantly suppresses mRNA expression of PXR and CAR by >60%, whereas presumed transcriptional regulators of UGT and CES enzymes are less impacted and FMO regulators are not at all impacted by cytokine treatment. Nuclear receptors and transcription factors implicated in DME transcriptional modulation are thus transcriptionally differentially regulated by cytokines, which might underlie the differential sensitivity to inflammation observed for various DME families. Besides inflammation-induced alterations in gene expression of regulators, a loss of nuclear localization or alterations in the phosphorylation status of regulators has also been proposed, i.e. for the dimerization partner RXRα (Ghose et al. 2004; Keller et al. 2016). This might explain the observed mismatch between the sensitivity towards pro-inflammatory cytokines for *CYP3A4* expression as compared to expression of the key regulators PXR and CAR. Future studies should aim to investigate whether the transcriptional downregulation concordantly leads to lower transcriptional activation of DME regulators.

Post-transcriptional mechanism related to inflammation may, alongside transcriptional changes, further affect CYP activity (Stanke-Labesque et al. 2020). For instance, nitric oxide-dependent ubiquitination leading to enhanced proteasomal degradation, or the release of inflammation-related miRNAs, have been implicated in this post-transcriptional regulatory process (Ferrari et al. 2001; Lee et al. 2009; Kugler et al. 2020). To investigate the importance of post-transcriptional mechanisms in modulating CYP activity under inflammatory conditions, we analyzed the correlation between the impact of IL-6 and IL-1β on DME expression versus DME activity. We found that, in HepaRG cells, alterations in gene

expression are highly predictive for alterations in enzyme activity, providing limited evidence for inflammation-associated post-transcriptional modifications of DMEs. Previous studies suggesting the importance of post-transcriptional modifications on CYP activity mainly stem from observed mismatches between mRNA and protein levels in PHHs (Aitken and Morgan 2007) or from animal studies (Stanke-Labesque et al. 2020). The time kinetics of alterations in expression versus protein/activity levels could partially account for the observed mismatches and future studies should therefore evaluate the temporal dynamics of DME expression and activity alterations in response to inflammation. We conducted our activity measurements after 72 hours, in accordance with other studies and considering the reported half-life of CYP3A4, which is approximately 37 hours (Willmann et al. 2003). However, half-life of CYP2C9 is reported to be 104 hours (Willmann et al. 2003), which could explain why we found a stronger effect of inflammation on *CYP2C9* expression compared to its activity. This finding is thus likely unrelated to post-transcriptional modifications but rather an effect of the protein's half-life. All in all, our results have highlighted that the transcriptional alterations in DME expression are the main driver of the alterations in enzyme activity observed *in vitro.*

PBPK modeling is increasingly exploited to predict the impact of inflammation or inflammatory diseases on drug clearance. A major advantage of PBPK modeling combined with *in vitro* to *in vivo* extrapolation (IVIVE) is the ability to translate *in vitro* data into biologically relevant parameters for model input to predict clinical inflammation-related alterations in pharmacokinetics. Specifically, IC_{50} and I_{max} values obtained *in vitro* can be used to model CYP enzyme dynamics under inflammatory conditions, and this approach has been shown successful for the prediction of disease-drug interactions with CYP substrates in for example patients with rheumatoid arthritis, leukemia or surgical trauma (Machavaram et al. 2013; Xu et al. 2015; Jiang et al. 2016; Machavaram et al. 2019; Lenoir et al. 2022). Despite the growing interest in PBPK modeling for non-CYP enzymes, current models predominantly focus on predicting drug-drug interactions rather than the impact of inflammation on non-CYP mediated drug clearance (Ozbey et al. 2023). This limitation arises

DMD Fast Forward. Published on September 30, 2024 as DOI: 10.1124/dmd.124.001867
This article has not been copyedited and formatted. The final version may differ from this version.

partly due to the scarcity of physiologically relevant quantitative *in vitro* data on the effects of cytokines on non-CYP enzymes (Kenny et al. 2013; Liu et al. 2023). To address this gap, we provided IC_{50} and I_{max} values for non-CYP enzymes, which can serve as critical inputs for PBPK modeling to better predict inflammation-related changes in non-CYP mediated drug metabolism. Importantly, comparing our HepaRG IL-6 IC_{50} values with those previously determined for CYP isoforms in 2D/3D PHHs showed good agreement between the results, enhancing our confidence in the validity of HepaRG data as input for PBPK modeling approaches. Also, our reported IC_{50} data are within the physiological range of serum IL-1β and IL-6 in patients experiencing inflammation-related diseases (Coutant and Hall 2018). Ultimately, PBPK models, when integrated with robust *in vitro* data, could serve as a powerful tool for optimizing drug dosing strategies and enhancing therapeutic outcomes in the presence of inflammation.

In the clinic, a differential impact of inflammation on DME family members has been observed, for example in non-alcoholic fatty liver disease (NAFLD) patients, where hepatic inflammation is an important contributor to disease progression (Song et al. 2023). Protein levels of CYPs were lower in diseased patients, but non-CYP enzyme levels remained relatively unchanged, except for select UGTs (Murphy et al. 2023). This was confirmed in another studies which showed CYP2C19 to be most impacted by NAFLD, whereas other DMEs were less affected (Powell et al. 2023; Govaere et al. 2024). For anti-fungal agents, a differential impact of inflammation has been demonstrated based on the metabolic route of the drug. Exposure of posaconazole, which is mainly metabolized by UGT1A4, was not influenced by inflammation as assessed by C-reactive protein (CRP) levels (Märtson et al. 2019). Conversely, different studies have demonstrated that trough levels of voriconazole, a substrate for CYP2C19/3A4, are increased during inflammation (Van Wanrooy et al. 2014; Veringa et al. 2017). As such, patients with inflammatory conditions may experience variation in pharmacokinetics of concomitant medication depending on the specific DME engaged in the drug's metabolic pathway. Our study suggests that drugs utilizing secondary or

alternative routes via non-CYP clearance may be less susceptible to the effects of inflammation as compared to drugs fully metabolized by CYP enzymes.

In conclusion, our study has shown that UGTs, FMOs and CESs enzymes are less sensitive towards the effects of pro-inflammatory cytokines IL-6 and IL-1β as compared to the CYP enzymes. Additionally, the findings highlight that transcriptional alterations in the DME expression are highly predictive for the alterations in enzyme activity, arguing against inflammation-related post-transcriptional modifications. Patients suffering from acute or chronic inflammatory diseases may thus be at risk for alterations in pharmacokinetics, where the magnitude of the alteration is likely depending on the DME family members involved in the clearance route of the drug.

Acknowledgement

The authors would like to thank and acknowledge Johan van der Reijden and Luuk Hawinkels (Department of Gastroenterology-Hepatology, Leiden University Medical Center) for their excellent support with acquiring and processing the human liver biopsies from the biobank.

Data availability statement

The authors declare that all the data supporting the findings of this study are available within the paper and its Supplemental Data

Author contributions

Participated in research design: de Jong, Harpal, Manson

Conducted experiments: de Jong, Harpal, van den Berg, Peter,

Performed data analysis: de Jong, Harpal, van den Berg, Hoekstra, Peter, Manson

Wrote or contributed to the writing of the manuscript: de Jong, Harpal, Hoekstra, Rissmann, Swen, Manson

References

Aitken AE, Morgan ET. 2007. Gene-specific effects of inflammatory cytokines on cytochrome P450 2C, 2B6 and 3A4 mRNA levels in human hepatocytes. Drug Metab Dispos. 35(9):1687–1693. doi:10.1124/dmd.107.015511.

Chen Y, Ferguson SS, Negishi M, Goldstein JA. 2003. Identification of constitutive androstane receptor and glucocorticoid receptor binding sites in the CYP2C19 promoter. Mol Pharmacol. 64(2):316–324. doi:10.1124/mol.64.2.316.

Chomczynski P, Sacchi N. 1987. Single-step method of RNA isolation by acid guanidinium thiocyanate-phenol-chloroform extraction. Anal Biochem. 162(1):156–159. doi:10.1006/ABIO.1987.9999.

Collins JM, Lu R, Wang X, Zhu HJ, Wang D. 2022. Transcriptional Regulation of Carboxylesterase 1 in Human Liver: Role of the Nuclear Receptor Subfamily 1 Group H Member 3 and Its Splice Isoforms. Drug Metab Dispos. 50(1):43–48. doi:10.1124/DMD.121.000649.

Court MH, Krishnaswamy S, Hao Q, Duan SX, Patten CJ, Von Moltke LL, Greenblatt DJ. 2003. Evaluation of 3'-azido-3'-deoxythymidine, morphine, and codeine as probe substrates for UDP-glucuronosyltransferase 2B7 (UGT2B7) in human liver microsomes: specificity and

influence of the UGT2B7*2 polymorphism. Drug Metab Dispos. 31(9):1125–1133. doi:10.1124/DMD.31.9.1125.

Coutant DE, Hall SD. 2018. Disease-Drug Interactions in Inflammatory States via Effects on CYP-Mediated Drug Clearance. J Clin Pharmacol. 58(7):849–863. doi:10.1002/JCPH.1093.

Dickmann LJ, Patel SK, C. Wienkers L, Greg Slatter J. 2012. Effects of Interleukin 1β (IL-1β) and IL-1β/Interleukin 6 (IL-6) Combinations on Drug Metabolizing Enzymes in Human Hepatocyte Culture. Curr Drug Metab. 13(7):930–937. doi:10.2174/138920012802138642.

Dickmann LJ, Patel SK, Rock DA, Wienkers LC, Slatter JG. 2011. Effects of interleukin-6 (IL-6) and an anti-IL-6 monoclonal antibody on drug-metabolizing enzymes in human hepatocyte culture. Drug Metab Dispos. 39(8):1415–1422. doi:10.1124/dmd.111.038679.

Dunvald ACD, Järvinen E, Mortensen C, Stage TB. 2022. Clinical and Molecular Perspectives on Inflammation-Mediated Regulation of Drug Metabolism and Transport. Clin Pharmacol Ther. 112(2):277–290. doi:10.1002/CPT.2432.

Ferguson SS, Lecluyse EL, Negishi M, Goldstein JA. 2002. Regulation of human CYP2C9 by the constitutive androstane receptor: Discovery of a new distal binding site. Mol Pharmacol. 62(3):737–746. doi:10.1124/mol.62.3.737.

Ferrari L, Peng N, Halpert JR, Morgan ET. 2001. Role of nitric oxide in down-regulation of CYP2B1 protein, but not RNA, in primary cultures of rat hepatocytes. Mol Pharmacol. 60(1):209–216. doi:10.1124/MOL.60.1.209.

Ghose R, Zimmerman TL, Thevananther S, Karpen SJ. 2004. Endotoxin leads to rapid subcellular re-localization of hepatic RXRalpha: A novel mechanism for reduced hepatic gene expression in inflammation. Nucl Recept. 2(1). doi:10.1186/1478-1336-2-4.

Govaere O, Cockell SJ, Zatorska M, Wonders K, Tiniakos D, Frey AM, Palmowksi P, Walker R, Porter A, Trost M, et al. 2024. Pharmacogene expression during progression of metabolic dysfunction-associated steatotic liver disease: Studies on mRNA and protein levels and their

relevance to drug treatment. Biochem Pharmacol. doi:10.1016/J.BCP.2024.116249.

Gramignoli R, Ranade AR, Venkataramanan R, Strom SC. 2022. Effects of Pro-Inflammatory Cytokines on Hepatic Metabolism in Primary Human Hepatocytes. Int J Mol Sci. 23(23). doi:10.3390/IJMS232314880.

Gripon P, Rumin S, Urban S, Le Seyec J, Glaise D, Cannie I, Guyomard C, Lucas J, Trepo C, Guguen-Guillouzo C. 2002. Infection of a human hepatoma cell line by hepatitis B virus. Proc Natl Acad Sci U S A. 99(24):15655–15660. doi:10.1073/PNAS.232137699.

Guillouzo A, Corlu A, Aninat C, Glaise D, Morel F, Guguen-Guillouzo C. 2007. The human hepatoma HepaRG cells: a highly differentiated model for studies of liver metabolism and toxicity of xenobiotics. Chem Biol Interact. 168(1):66–73. doi:10.1016/J.CBI.2006.12.003.

Hines RN. 2006. Developmental and tissue-specific expression of human flavin-containing monooxygenases 1 and 3. Expert Opin Drug Metab Toxicol. 2(1):41–49. doi:10.1517/17425255.2.1.41.

Hu DG, Meech R, McKinnon RA, Mackenzie PI. 2014. Transcriptional regulation of human UDP-glucuronosyltransferase genes. Drug Metab Rev. 46(4):421–458. doi:10.3109/03602532.2014.973037.

Izukawa T, Nakajima M, Fujiwara R, Yamanaka H, Fukami T, Takamiya M, Aoki Y, Ikushiro SI, Sakaki T, Yokoi T. 2009. Quantitative analysis of UDP-glucuronosyltransferase (UGT) 1A and UGT2B expression levels in human livers. Drug Metab Dispos. 37(8):1759–1768. doi:10.1124/DMD.109.027227.

Jablonska E, Jablonski J, Piotrowski L, Grabowska Z. 2001. IL-1beta, IL-1Ra and sIL-1RII in the culture supernatants of PMN and PBMC and the serum levels in patients with inflammation and patients with cancer disease of the same location. Immunobiology. 204(4):508–516. doi:10.1078/0171-2985-00059.

Jiang X, Zhuang Y, Xu Z, Wang W, Zhou H. 2016. Development of a Physiologically Based

Pharmacokinetic Model to Predict Disease-Mediated Therapeutic Protein-Drug Interactions: Modulation of Multiple Cytochrome P450 Enzymes by Interleukin-6. AAPS J. 18(3):767–776. doi:10.1208/S12248-016-9890-5.

de Jong LM, Boussallami S, Sánchez-López E, Giera M, Tushuizen ME, Hoekstra M, Hawinkels LJAC, Rissmann R, Swen JJ, Manson ML. 2023. The impact of CYP2C19 genotype on phenoconversion by concomitant medication. Front Pharmacol. 14. doi:10.3389/FPHAR.2023.1201906.

de Jong LM, Jiskoot W, Swen JJ, Manson ML. 2020. Distinct effects of inflammation on cytochrome P450 regulation and drug metabolism: Lessons from experimental models and a potential role for pharmacogenetics. Genes (Basel). 11(12):1–24. doi:10.3390/GENES11121509.

Keller R, Klein M, Thomas M, Dräger A, Metzger U, Templin MF, Joos TO, Thasler WE, Zell A, Zanger UM. 2016. Coordinating Role of RXRα in Downregulating Hepatic Detoxification during Inflammation Revealed by Fuzzy-Logic Modeling. Altan-Bonnet G, editor. PLOS Comput Biol. 12(1):e1004431. doi:10.1371/journal.pcbi.1004431.

Kenny JR, Liu MM, Chow AT, Earp JC, Evers R, Slatter JG, Wang DD, Zhang L, Zhou H. 2013. Therapeutic protein drug-drug interactions: navigating the knowledge gaps-highlights from the 2012 AAPS NBC Roundtable and IQ Consortium/FDA workshop. AAPS J. 15(4):933–940. doi:10.1208/S12248-013-9495-1.

Kiamehr M, Heiskanen L, Laufer T, Düsterloh A, Kahraman M, Käkelä R, Laaksonen R, Aalto-Setälä K. 2019. Dedifferentiation of Primary Hepatocytes is Accompanied with Reorganization of Lipid Metabolism Indicated by Altered Molecular Lipid and miRNA Profiles. Int J Mol Sci. 20(12). doi:10.3390/IJMS20122910.

Klein K, Zanger UM. 2013. Pharmacogenomics of Cytochrome P450 3A4: Recent Progress Toward the “Missing Heritability” Problem. Front Genet. 4(FEB). doi:10.3389/FGENE.2013.00012.

Klein M, Thomas M, Hofmann U, Seehofer D, Damm G, Zanger UM. 2015. A systematic comparison of the impact of inflammatory signaling on absorption, distribution, metabolism, and excretion gene expression and activity in primary human hepatocytes and HepaRG Cells. Drug Metab Dispos. 43(2):273–283. doi:10.1124/dmd.114.060962.

Klick DE, Hines RN. 2007. Mechanisms regulating human FMO3 transcription. Drug Metab Rev. 39(2–3):419–442. doi:10.1080/03602530701498612.

Klöditz K, Tewolde E, Nordling Å, Ingelman-Sundberg M. 2023. Mechanistic, Functional, and Clinical Aspects of Pro-inflammatory Cytokine Mediated Regulation of ADME Gene Expression in 3D Human Liver Spheroids. Clin Pharmacol Ther. 114(3):673–685. doi:10.1002/CPT.2969.

Kugler N, Klein K, Zanger UM. 2020. MiR-155 and other microRNAs downregulate drug metabolizing cytochromes P450 in inflammation. Biochem Pharmacol. 171. doi:10.1016/J.BCP.2019.113725.

Lee CM, Pohl J, Morgan ET. 2009. Dual mechanisms of CYP3A protein regulation by proinflammatory cytokine stimulation in primary hepatocyte cultures. Drug Metab Dispos. 37(4):865–872. doi:10.1124/DMD.108.026187.

Lenoir C, Niederer A, Rollason V, Desmeules JA, Daali Y, Samer CF. 2022. Prediction of cytochromes P450 3A and 2C19 modulation by both inflammation and drug interactions using physiologically based pharmacokinetics. CPT pharmacometrics Syst Pharmacol. 11(1):30–43. doi:10.1002/PSP4.12730.

Leung JG, Nelson S, Takala CR, Gören JL. 2014. Infection and inflammation leading to clozapine toxicity and intensive care: a case series. Ann Pharmacother. 48(6):801–805. doi:10.1177/1060028014526701.

Liu F, Aulin LBS, Manson ML, Krekels EHJ, van Hasselt JGC. 2023. Unraveling the Effects of Acute Inflammation on Pharmacokinetics: A Model-Based Analysis Focusing on Renal

Glomerular Filtration Rate and Cytochrome P450 3A4-Mediated Metabolism. Eur J Drug Metab Pharmacokinet. 48(6):623–631. doi:10.1007/S13318-023-00852-6.

Livak KJ, Schmittgen TD. 2001. Analysis of relative gene expression data using real-time quantitative PCR and the 2(-Delta Delta C(T)) Method. Methods. 25(4):402–408. doi:10.1006/METH.2001.1262.

Machavaram KK, Almond LM, Rostami-Hodjegan A, Gardner I, Jamei M, Tay S, Wong S, Joshi A, Kenny JR. 2013. A physiologically based pharmacokinetic modeling approach to predict disease-drug interactions: Suppression of CYP3A by IL-6. Clin Pharmacol Ther. 94(2):260–268. doi:10.1038/clpt.2013.79.

Machavaram KK, Endo-Tsukude C, Terao K, Gill KL, Hatley OJ, Gardner I, Parrott N, Ducray PS. 2019. Simulating the Impact of Elevated Levels of Interleukin-6 on the Pharmacokinetics of Various CYP450 Substrates in Patients with Neuromyelitis Optica or Neuromyelitis Optica Spectrum Disorders in Different Ethnic Populations. AAPS J. 21(3). doi:10.1208/s12248-019-0309-y.

Märtson AG, Veringa A, Bakker M, van den Heuvel ER, Touw DJ, van der Werf TS, Span LFR, C. Alffenaar JW. 2019. Posaconazole trough concentrations are not influenced by inflammation: A prospective study. Int J Antimicrob Agents. 53(3):325–329. doi:10.1016/J.IJANTIMICAG.2019.01.006.

Murphy WA, Adiwidjaja J, Sjöstedt N, Yang K, Beaudoin JJ, Spires J, Siler SQ, Neuhoff S, Brouwer KLR. 2023. Considerations for Physiologically Based Modeling in Liver Disease: From Nonalcoholic Fatty Liver (NAFL) to Nonalcoholic Steatohepatitis (NASH). Clin Pharmacol Ther. 113(2):275–297. doi:10.1002/CPT.2614.

Nguyen T V., Ukairo O, Khetani SR, McVay M, Kanchagar C, Seghezzi W, Ayanoglu G, Irrechukwu O, Evers R. 2015. Establishment of a hepatocyte-kupffer cell coculture model for assessment of proinflammatory cytokine effects on metabolizing enzymes and drug transporters. Drug Metab Dispos. 43(5):774–785. doi:10.1124/dmd.114.061317.

Ozbey AC, Fowler S, Leys K, Annaert P, Umehara K, Parrott N. 2023. PBPK Modelling for Drugs Cleared by Non-CYP Enzymes: State-of-the-Art and Future Perspectives. Drug Metab Dispos. 52(1):44–55. doi:10.1124/DMD.123.001487.

Pinto C, Giordano DM, Maroni L, Marzioni M. 2018. Role of inflammation and proinflammatory cytokines in cholangiocyte pathophysiology. Biochim Biophys acta Mol basis Dis. 1864(4 Pt B):1270–1278. doi:10.1016/J.BBADIS.2017.07.024.

Powell NR, Liang T, Ipe J, Cao S, Skaar TC, Desta Z, Qian HR, Ebert PJ, Chen Y, Thomas MK, et al. 2023. Clinically important alterations in pharmacogene expression in histologically severe nonalcoholic fatty liver disease. Nat Commun. 14(1). doi:10.1038/S41467-023-37209-1.

Saravanakumar A, Sadighi A, Ryu R, Akhlaghi F. 2019. Physicochemical Properties, Biotransformation, and Transport Pathways of Established and Newly Approved Medications: A Systematic Review of the Top 200 Most Prescribed Drugs vs. the FDA-Approved Drugs Between 2005 and 2016. Clin Pharmacokinet. 58(10):1281–1294. doi:10.1007/S40262-019-00750-8.

Schaper F, Rose-John S. 2015. Interleukin-6: Biology, signaling and strategies of blockade. Cytokine Growth Factor Rev. 26(5):475–487. doi:10.1016/J.CYTOGFR.2015.07.004.

Sebaugh JL. 2011. Guidelines for accurate EC50/IC50 estimation. Pharm Stat. 10(2):128–134. doi:10.1002/PST.426.

Song C, Long X, He J, Huang Y. 2023. Recent evaluation about inflammatory mechanisms in nonalcoholic fatty liver disease. Front Pharmacol. 14. doi:10.3389/FPHAR.2023.1081334.

Spaggiari D, Geiser L, Daali Y, Rudaz S. 2014. A cocktail approach for assessing the in vitro activity of human cytochrome P450s: an overview of current methodologies. J Pharm Biomed Anal. 101:221–237. doi:10.1016/J.JPBA.2014.03.018.

Stader F, Battegay M, Sendi P, Marzolini C. 2022. Physiologically Based Pharmacokinetic

Modelling to Investigate the Impact of the Cytokine Storm on CYP3A Drug Pharmacokinetics in COVID-19 Patients. Clin Pharmacol Ther. 111(3):579–584. doi:10.1002/CPT.2402.

Stanke-Labesque F, Gautier-Veyret E, Chhun S, Guilhaumou R. 2020. Inflammation is a major regulator of drug metabolizing enzymes and transporters: Consequences for the personalization of drug treatment. Pharmacol Ther. 215. doi:10.1016/J.PHARMTHERA.2020.107627.

Störmer E, Roots I, Brockmöller J. 2000. Benzydamine N-oxidation as an index reaction reflecting FMO activity in human liver microsomes and impact of FMO3 polymorphisms on enzyme activity. Br J Clin Pharmacol. 50(6):553–561. doi:10.1046/J.1365-2125.2000.00296.X.

Tanner N, Kubik L, Luckert C, Thomas M, Hofmann U, Zanger UM, Böhmert L, Lampen A, Braeuning A. 2018. Regulation of Drug Metabolism by the Interplay of Inflammatory Signaling, Steatosis, and Xeno-Sensing Receptors in HepaRG Cells. Drug Metab Dispos. 46(4):326–335. doi:10.1124/DMD.117.078675.

Veringa A, ter Avest M, Span LFR, van den Heuvel ER, Touw DJ, Zijlstra JG, Kosterink JGW, van der Werf TS, Alffenaar JWC. 2017. Voriconazole metabolism is influenced by severe inflammation: A prospective study. J Antimicrob Chemother. 72(1):261–267. doi:10.1093/jac/dkw349.

Van Wanrooy MJP, Span LFR, Rodgers MGG, Van Heuvel ERD, Uges DRA, Van Werf TSD, Kosterink JGW, Alffenaara JWC. 2014. Inflammation is associated with voriconazole trough concentrations. Antimicrob Agents Chemother. 58(12):7098–7101. doi:10.1128/AAC.03820-14.

Weber A, Wasiliew P, Kracht M. 2010. Interleukin-1 (IL-1) pathway. Sci Signal. 3(105). doi:10.1126/SCISIGNAL.3105CM1.

Willmann S, Lippert J, Sevestre M, Solodenko J, Fois F, Schmitt W. 2003. PK-Sim®: A

physiologically based pharmacokinetic “whole-body” model. Drug Discov Today BIOSILICO. 1(4):121–124. doi:10.1016/S1478-5382(03)02342-4.

Xie W, Barwick JL, Simon CM, Pierce AM, Safe S, Blumberg B, Guzelian PS, Evans RM. 2000. Reciprocal activation of xenobiotic response genes by nuclear receptors SXR/PXR and CAR. Genes Dev. 14(23):3014–3023. doi:10.1101/gad.846800.

Xu Y, Hijazi Y, Wolf A, Wu B, Sun YN, Zhu M. 2015. Physiologically Based Pharmacokinetic Model to Assess the Influence of Blinatumomab-Mediated Cytokine Elevations on Cytochrome P450 Enzyme Activity. CPT pharmacometrics Syst Pharmacol. 4(9):507–515. doi:10.1002/PSP4.12003.

Zanger UM, Schwab M. 2013. Cytochrome P450 enzymes in drug metabolism: regulation of gene expression, enzyme activities, and impact of genetic variation. Pharmacol Ther. 138(1):103–141. doi:10.1016/J.PHARMTHERA.2012.12.007.

Footnotes

No funding was received for this work

The authors declare that there are no conflicts of interest

DMD Fast Forward. Published on September 30, 2024 as DOI: 10.1124/dmd.124.001867
This article has not been copyedited and formatted. The final version may differ from this version.

Figure legends

Figure 1. Basal mRNA expression levels of phase I and phase II drug metabolizing enzymes in HepaRG cells and in human livers. mRNA expression of the gene of interest was normalized to the housekeeping gene *RPLP0* and presented as a fold change compared to basal *CYP3A4* expression of either HepaRG cells or human livers. All values are means + SEM from 8 independent experiments (HepaRG) or from biopsies of 40 human livers.

Figure 2. Cytokine concentration-response curves for regulation of CYP isoforms CYP3A4, CYP2C9, CYP2C19, CYP1A2 on expression (A) and activity level (B). Cells were treated with concentrations of 0.0001 ng/mL to 10 ng/mL (IL-6) or 0.001 pg/mL to 1 ng/mL (IL-1β) for 24 hours to analyze gene expression alterations via RT-qPCR or for 72 hours to analyze activity alterations via probe substrate metabolism with LC-MS/MS. mRNA and activity data are expressed as fold change of levels found in untreated control cells, arbitrarily set to 1.0. Each data point represents the average ± SEM of at least 4 independent experiments. Data were fit with a non-linear regression model.

Figure 3. Cytokine concentration-response curves for regulation of CYP3A4, FMO3, UGT2B7 and CES1 on expression (A) and activity level (B). Cells were treated with concentrations of 0.0001 ng/mL to 10 ng/mL (IL-6) or 0.001 pg/mL to 1 ng/mL (IL-1β) for 24 hours to analyze gene expression alterations via RT-qPCR or for 72 hours to analyze activity alterations via probe substrate metabolism with LC-MS/MS. mRNA and activity data are expressed as fold changes of levels found in untreated control cells, arbitrarily set to 1.0. Each data point represents the average ± SEM of at least 4 independent experiments. Data were fit with a non-linear regression model.

Figure 4. Simple linear regression analysis to investigate the relationship between the impact of IL-6 and IL-1β treatment on DME mRNA expression versus activity for $LogIC_{50}$ values (A) and I_{max} values (B). The regression line represents the best-fit line calculated from the data, and the dotted lines indicate the 95% confidence interval. Blue dots represent data obtained from IL-6 treated cells, and brown dots represent data obtained from IL-1β treated cells.

Figure 5. The impact of IL-6 or IL-1β on transcription factors and nuclear receptors that regulate the various DMEs families. Cells were treated with 10 ng/mL IL-6 or 1 ng/mL IL-1β for 24 hours to analyze gene expression alterations via RT-qPCR. Data are expressed as the mean fold change ± SEM of

mRNA compared to untreated control cells of 6 independent experiments. One way ANOVA with Dunnett post hoc test was performed for every gene separately. ** P<0.01, *** P<0.001.

DMD Fast Forward. Published on September 30, 2024 as DOI: 10.1124/dmd.124.001867
This article has not been copyedited and formatted. The final version may differ from this version.

Tables

Table 1. Quantified IC_{50} and I_{max} values for DME mRNA expression levels obtained from fitting a non-linear regression model on the concentration-effect curves after treatment with IL-6 or IL-1β for 24 hours. The IC_{50} values are reported in ng/mL for IL-6 treatment and in pg/mL for IL-1β treatment. One-way ANOVA and Dunnett's post hoc test with comparison to *CYP3A4* was done to investigate differences in potency and maximal effect between DME families, for both IL-6 and IL-1β treatment. * P<0.05, ** P<0.01, *** P<0.001.

	IL-6		IL-1β	
	Potency (IC_{50}, ng/mL) ± SD	**Maximal effect (I_{max}) ± SD (%)**	**Potency (IC_{50}, pg/mL) ± SD**	**Maximal effect (I_{max}) ± SD (%)**
CYP3A4	0.14 ± 0.10	97 ± 1	0.35 ± 0.94	99 ± 2
CYP1A2	0.04 ± 0.22	94 ± 3	0.24 ± 1.02	99 ± 1
CYP2C9	0.41 ± 0.29	82 ± 6	0.90 ± 2.05	94 ± 4
CYP2C19	0.27 ± 0.47	86 ± 5	0.98 ± 1.23	94 ± 6
FMO1	0.57 ± 0.22	84 ± 11	1.80 ± 4.47	97 ± 3
FMO3	1.00 ± 1.86**	55 ± 9***	6.15 ± 12.10**	84 ± 6**
FMO4	1.07 ± 0.95**	57 ± 4***	9.95 ± 13.56***	80 ± 3***
CES1	1.23 ± 0.30**	39 ± 15***	no effect	no effect
CES2	0.70 ± 0.30*	48 ± 13***	10.67 ± 9.32**	84 ± 1*
UGT1A4	0.61 ± 0.88*	68 ± 17***	1.93 ± 7.63	84 ± 17**
UGT2B4	0.76 ± 0.58*	73 ± 7***	3.28 ± 14.19*	94 ± 4
UGT2B7	1.05 ± 0.42 **	60 ± 12***	5.01 ± 17.97**	83 ± 10***
UGT2B15	0.59 ± 0.30	72 ± 13***	1.53 ± 6.55	97 ± 2

DMD Fast Forward. Published on September 30, 2024 as DOI: 10.1124/dmd.124.001867
This article has not been copyedited and formatted. The final version may differ from this version.

Table 2. Quantified IC_{50} and I_{max} values for DME activity obtained from fitting a non-linear regression model on the concentration-effect curves after treatment with IL-6 or IL-1β for 72 hours. The IC_{50} values are reported in ng/mL for IL-6 treatment and in pg/mL for IL-1β treatment. One-way ANOVA and Dunnett's post hoc test with comparison to CYP3A4 was done to investigate differences in potency and efficacy between DME families, for both IL-6 and IL-1β. * P<0.05, ** P<0.01, *** P<0.001.

	Activity			
	IL-6		IL-1β	
	Potency (IC_{50}, ng/mL) ± SD	**Maximal decrease (I_{max}) ± SD (%)**	**Potency (IC_{50}, pg/mL) ± SD**	**Maximal decrease (I_{max}) ± SD (%)**
CYP3A4	0.05 ± 0.17	93 ± 2	0.60 ± 2.31	98 ± 1
CYP1A2	0.12 ± 0.11	85 ± 4*	0.43 ± 3.55	89 ± 1***
CYP2C9	0.55 ± 0.36***	89 ± 3	4.82 ± 4.59*	93 ± 3**
CYP2C19	0.52 ± 0.17***	89 ± 2	6.58 ± 6.27*	99 ± 0
FMO3	1.28 ± 1.82***	29 ± 5***	1.49 ± 0.43	54 ± 5***
UGT2B7	1.77 ± 0.71***	69 ± 7***	18.48 ± 15.54**	93 ± 2*

DMD Fast Forward. Published on September 30, 2024 as DOI: 10.1124/dmd.124.001867
This article has not been copyedited and formatted. The final version may differ from this version.

Table 3. Quantified IC_{50} values in HepaRG cells from this study as compared to reported values in 2D and 3D PHH models. Data from 3D PHH models was extracted from the publication by Klöditz *et al.* (2023) and represents the average of 4 independent donors. Data from 2D PHHs was extracted from the studies by Dickmann *et al.* (2011, 2012) and represents the average of 5 independent donors unless stated otherwise.

	IL-6						IL-1β					
	HepaRG (IC_{50}, ng/mL)		**3D PHH (IC_{50}, ng/mL)**		**2D PHH (IC_{50}, ng/mL)**		**HepaRG (IC_{50}, ng/mL)**		**3D PHH (IC_{50}, ng/mL)**		**2D PHH (IC_{50}, ng/mL)**	
	mRNA	**Activity**	**mRNA**	**Activity**	**mRNA[#]**	**Activity**	**mRNA**	**Activity**	**mRNA**	**Activity**	**mRNA**	**Activity**
CYP3A4	0.14	0.05	0.46	N.D.	0.003	0.07	0.0004	0.0006	0.02	N.D.	0.29	0.42
CYP1A2	0.04	0.12	0.03	N.D.	0.27	1.25	0.0002	0.0004	0.60	N.D.	0.53[###]	0.45[##]
CYP2C9	0.41	0.55	0.20	N.D.	0.12	N.D.	0.0009	0.0048	3.95	N.D.	0.23	N.D.
CYP2C19	0.27	0.52	0.25	N.D.	0.07	N.D.	0.0010	0.0066	0.42	N.D.	0.15[###]	N.D.

N.D. = not determined.

[#]data from one donor, [##] could only be measured in 2 out of 5 donors, [###]could only be measured in 3 out of 5 donors.

Fig. 1

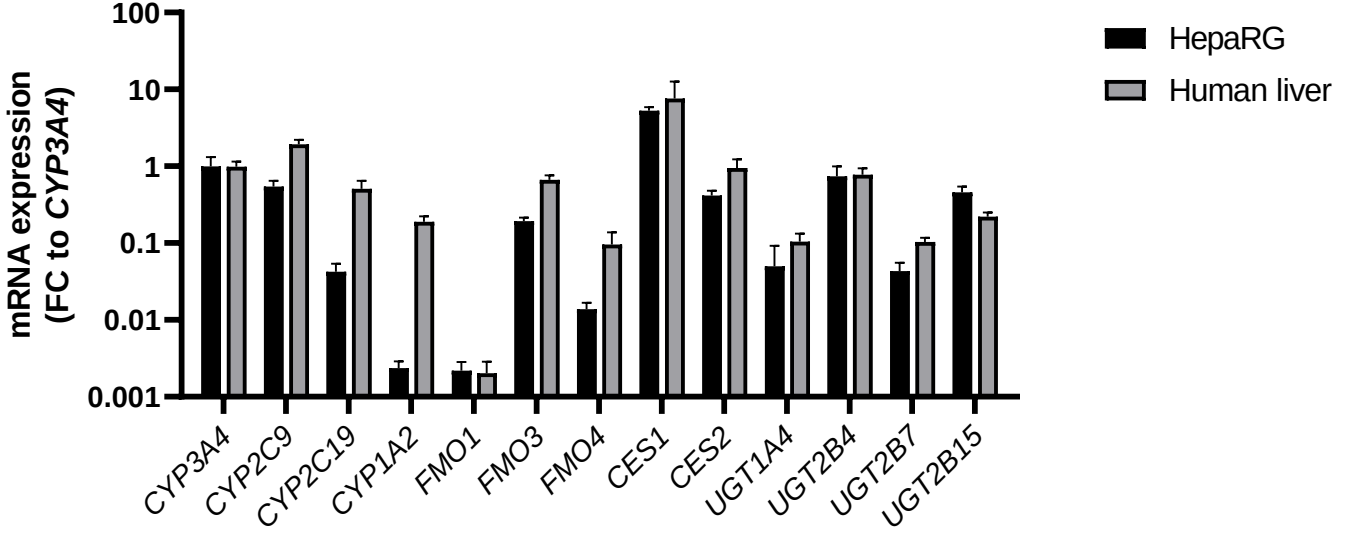

Fig. 2

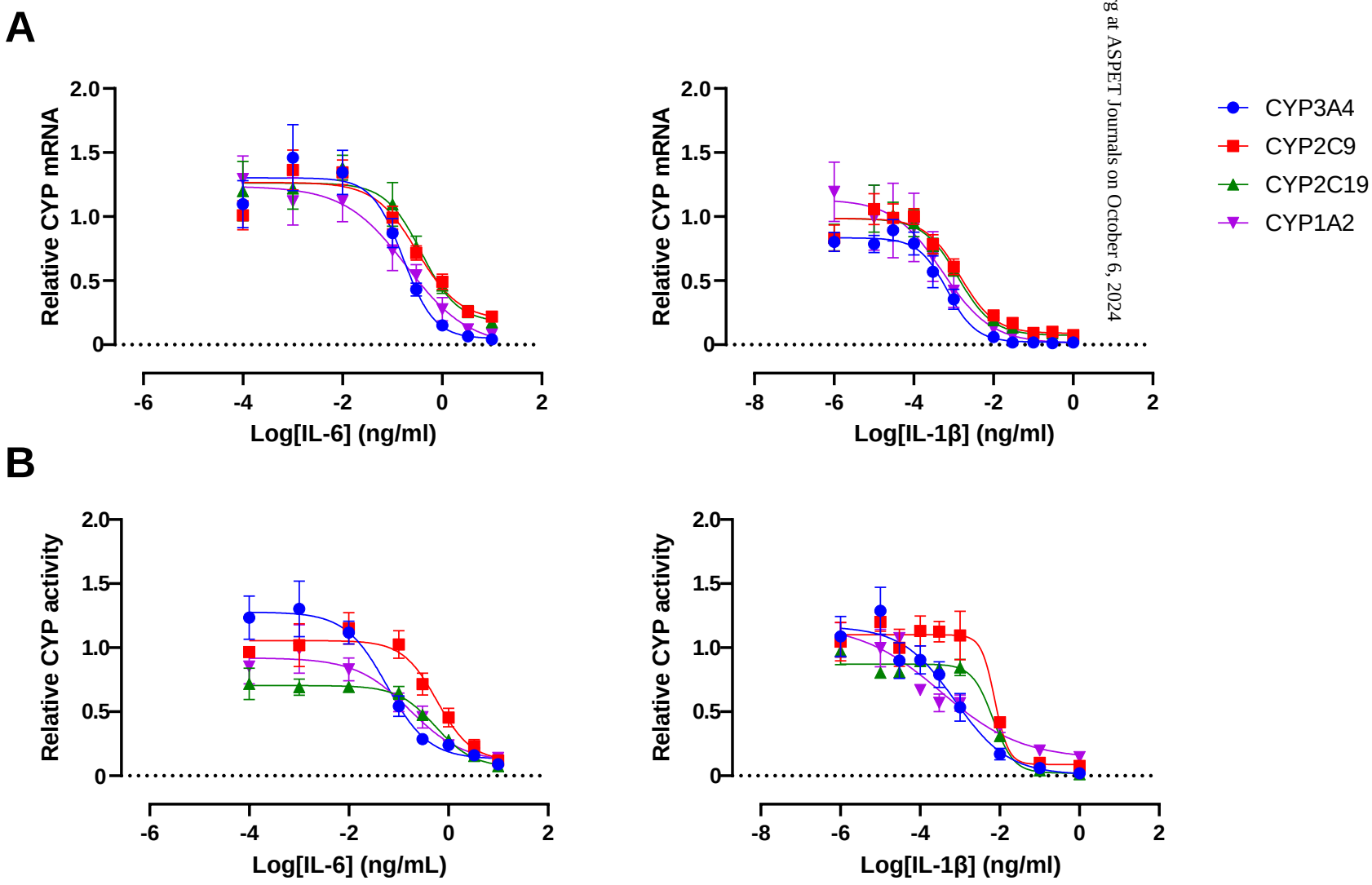

Fig. 3

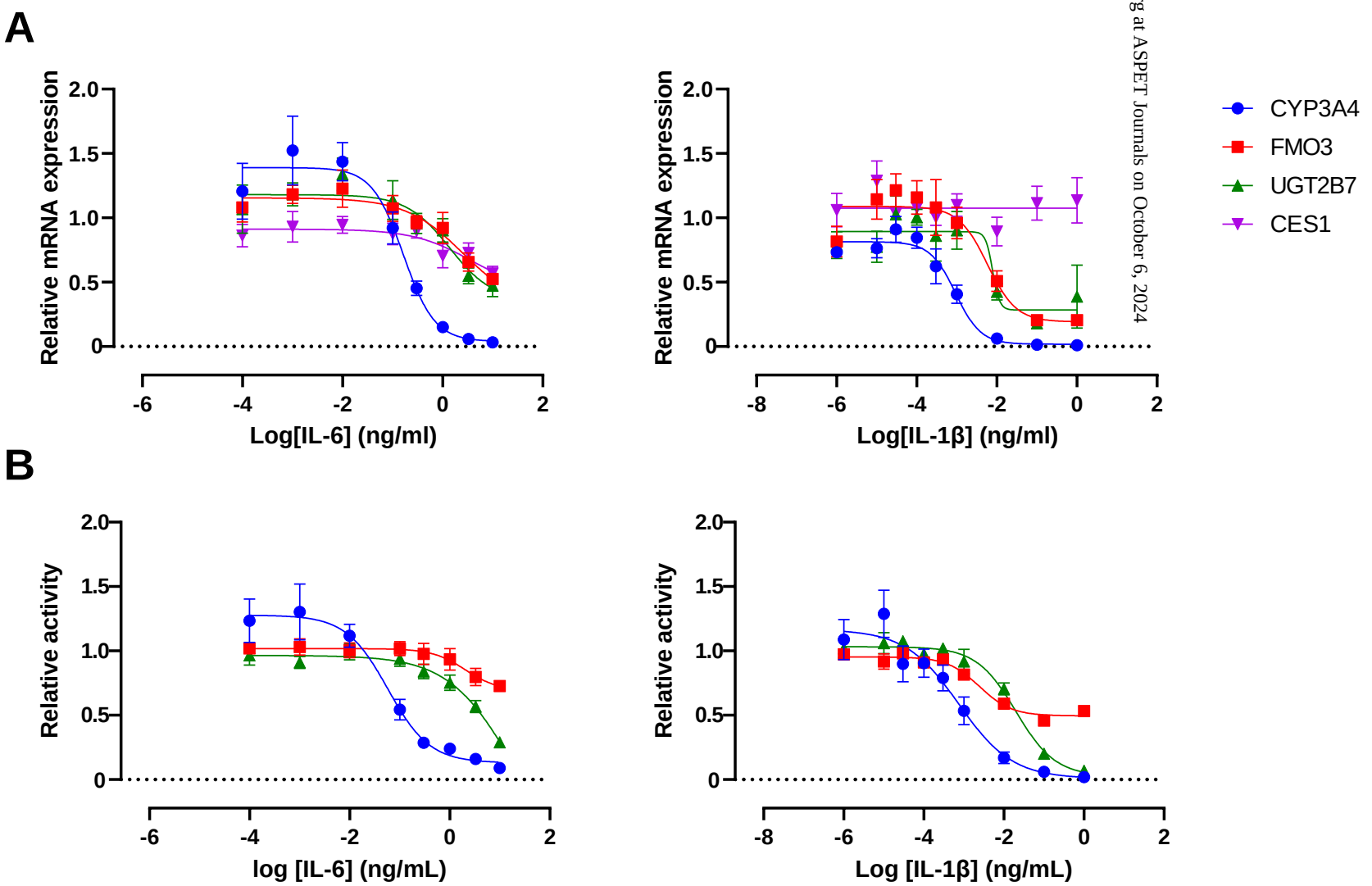

Fig. 4

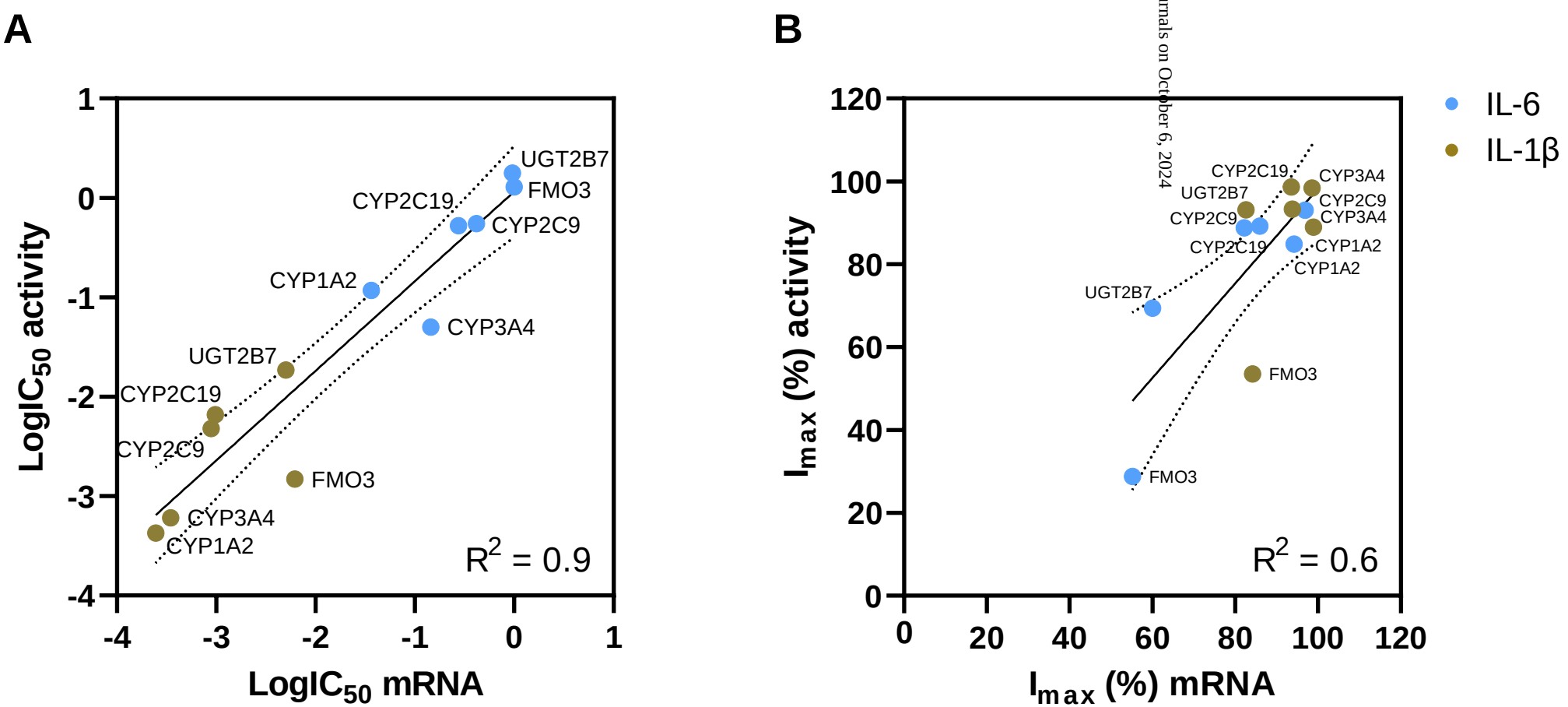

Fig. 5